Discovery of Novel 1,3,8-Triazaspiro[4.5]decane Derivatives That Target the c Subunit of F$_1$/F$_O$-Adenosine Triphosphate (ATP) Synthase for the Treatment of Reperfusion Damage in Myocardial Infarction

Giampaolo Morciano,[†,‡,§,∥,$] Delia Preti,[⊥,$] Gaia Pedriali,[‡,§,∥,$] Giorgio Aquila,[#] Sonia Missiroli,[§,∥] Anna Fantinati,[⊥] Natascia Caroccia,[§,∥] Salvatore Pacifico,[⊥] Massimo Bonora,[§,∥] Anna Talarico,[⊥] Claudia Morganti,[§,∥] Paola Rizzo,[‡,§] Roberto Ferrari,[‡,§,∇] Mariusz R. Wieckowski,[◇] Gianluca Campo,[‡,∇] Carlotta Giorgi,[§,∥] Claudio Trapella,*[∥,⊥] and Paolo Pinton*[‡,§,∥] [ORCID]

[†]Maria Pia Hospital, GVM Care & Research, 10132, Torino, Italy
[‡]Maria Cecilia Hospital, GVM Care & Research, 48033, Cotignola, Ravenna, Italy
[§]Department of Morphology, Surgery and Experimental Medicine, Section of Pathology, Oncology and Experimental Biology,
[∥]Laboratory for Technologies of Advanced Therapies (LTTA), [⊥]Department of Chemical and Pharmaceutical Sciences, and
[#]Department of Medical Sciences, University of Ferrara, Ferrara 44121, Italy
[∇]Cardiovascular Institute, Azienda Ospedaliera-Universitaria S. Anna, Cona, Ferrara 44121, Italy
[◇]Department of Biochemistry, Nencki Institute of Experimental Biology, Polish Academy of Sciences, Warsaw 02-093, Poland

[S] *Supporting Information*

ABSTRACT: Recent cardiology research studies have reported the role, function, and structure of the mitochondrial permeability transition pore (mPTP) and have shown that its opening plays a key role in the progression of myocardial cell death secondary to reperfusion. In this manuscript, we validated a new pharmacological approach as an adjunct to reperfusion in myocardial infarction (MI) treatment and describe the discovery, optimization, and structure−activity relationship (SAR) studies of the first small-molecule mPTP opening inhibitors based on a 1,3,8-triazaspiro[4.5]decane scaffold that targets the c subunit of the F$_1$/F$_O$-ATP synthase complex. We identified three potential compounds with good mPTP inhibitory activity and beneficial

effects in a model of MI, including a decreased apoptotic rate in the whole heart and overall improvement of cardiac function upon administration during reperfusion. The selected compounds did not show off-target effects at the cellular and mitochondrial levels. Moreover, the compounds preserved the mitochondrial ATP content despite interacting with the ATP synthase complex.
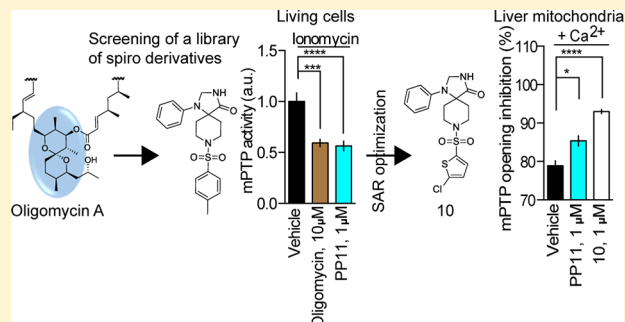
INTRODUCTION

Programmed cell death (PCD) is a physiological, evolutionarily conserved event that is essential for both intrauterine and postembryonic development as well as tissue homeostasis through elimination of damaged cells.[1] In humans, excessive PCD may be the basis of many diseases, including cardiovascular and neurodegenerative disorders. Several types of PCD exist, including mitochondrial permeability transition (MPT)-driven apoptosis,[2] during which the inner mitochondrial membrane (IMM), which is typically highly impermeable, exhibits increased permeability with a consequent osmotic influx of solutes in the mitochondrial matrix followed by loss of structural and functional characteristics of the affected mitochondria.[3] This MPT state is considered to be mediated by the mitochondrial permeability transition pore complex

(PTPC), a membrane multiprotein platform composed of a pore-forming part(s) and modulators that contribute to its conformational state and thus its mechanism of action.[4] Conditions favoring mitochondrial permeability transition pore (mPTP) opening include increased intramitochondrial calcium concentrations ([Ca^{2+}]), oxidative stress, and phosphates as well as high pH levels, all of which occur in ischemia−reperfusion-based injuries.[5,6]

Although many components/modulators of the mPTP have been discovered in recent years,[7,8] the proteins involved in the channel-forming fraction are still under intensive investigation. In two previous studies,[9,10] we provided experimental evidence
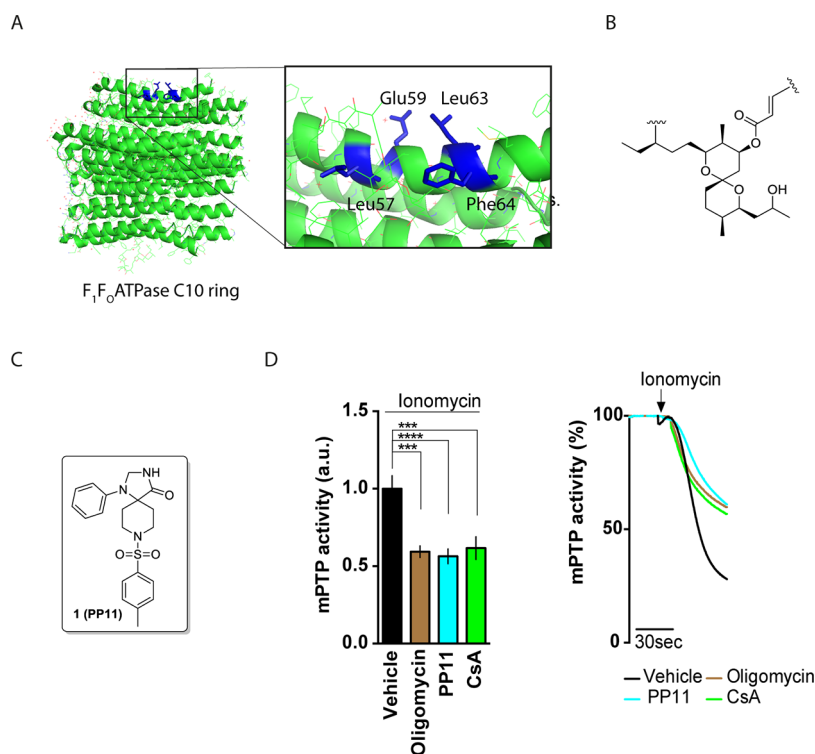
Figure 1. Discovery of PP11 as the first small-molecule inhibitor of the mPTP with a spirocenter template that mimics the spiroketal moiety of oligomycin A. (A) Graphical representation of the key amino acid residues defining the binding pocket of the known mPTP inhibitor oligomycin A to the c ring. (B) Structure of the southern portion of oligomycin A showing a 1,7-dioxaspiro[5.5]undecan moiety that is closely involved in the interaction with the c ring. (C) Structure of PP11, a novel small-molecule inhibitor of the mPTP with a 1,3,8-triaza-spiro[4.5]decan-4-one template. (D) Calcein−cobalt assay in living cells pretreated with vehicle, oligomycin A, PP11, and CsA. mPTP opening was stimulated by ionomycin administration, and representative kinetics data are reported. (***) p value < 0.001. (****) p value < 0.0001. CsA: cyclosporine A.

that the c subunit of F_1/F_O-ATP synthase plays a pivotal role in mPTP activity and mPTP formation, demonstrating a strong correlation between the mPTP functional state and c subunit expression; indeed, depletion of the c subunit reduced channel opening in response to calcium- and oxidative stress-induced stimuli, whereas its overexpression enhanced mPTP opening.[9] Contrary to what was proposed by another study,[11] we previously showed that the MPT is linked to the dissociation of F_1/F_O-ATP synthase dimers. Moreover, a proper c-ring conformation is required for MPT induction once F_1/F_O-ATP synthase dimers have dissociated.[10] Other independent groups have confirmed and extended our observations, defining the dissociation of F_1 from F_O during the MPT and recording a leak conductance within the purified c subunit ring that may form the channel of the mPTP.[12−15] Indeed, major evidence for the so-called "c-ring hypothesis" is derived from a comparison between a recent description of a voltage-sensitive pore represented by reconstituted c subunit proteins and lacking cation selectivity[12] and the multiconductance channel studied in the 1980−1990s,[16] where c rings may be exposed during F_1/F_O uncoupling.[12] However, these theories are not entirely supported by in silico simulations,[17] and mathematical calculations may not have considered other regulatory proteins that facilitate the channel formation process.[14]

While extensive effort has been invested in the synthesis and testing of new mPTP opening inhibitors,[18,19] to the best of our knowledge, none of these inhibitors were designed to target the c subunit expressed in eukaryotic cells or for cardioprotective purposes in the treatment of myocardial infarction (MI); however, Danshensu (DSS), which is isolated

from a traditional Chinese herb, is reported to modulate c subunit protein expression and have cell-protective effects.[20]

Among ATP synthase inhibitors, oligomycin A was identified in 1958.[21] Its presence is sensed by a subunit important for the functional and structural coupling between F_O and F_1: the oligomycin sensitivity-conferring protein (OSCP). Recently, an important role of OSCP as a site of interaction with cyclophilin (CyP) D, a matrix protein that can modulate mPTP opening, was discovered. Intriguingly, in the early 2000s, two reports described the potential of oligomycin A to inhibit mPTP opening induced by selenite[22] and its additive effect on cyclosporine A (CsA)-dependent mPTP activity.[23] Therefore, in addition to the finding that oligomycin A binds to the c ring of yeast mitochondrial ATP synthase as shown in an high-resolution crystal structure model,[24] this compound increased the protective effects against MPT conferred by F_1/F_O-ATP synthase, again demonstrating its role in membrane permeability.

With the aim of identifying a new pharmacological approach for the treatment of ischemia−reperfusion-related damage, in this manuscript, we describe the discovery, optimization, and structure−activity relationship (SAR) studies of the first small-molecule mPTP inhibitors to target the c subunit of the F_1/F_O-ATP synthase complex. These compounds, which are based on a 1,3,8-triazaspiro[4.5]decane scaffold, may lead to the development of new cardio/neuroprotective agents for the clinical management of ischemic events.
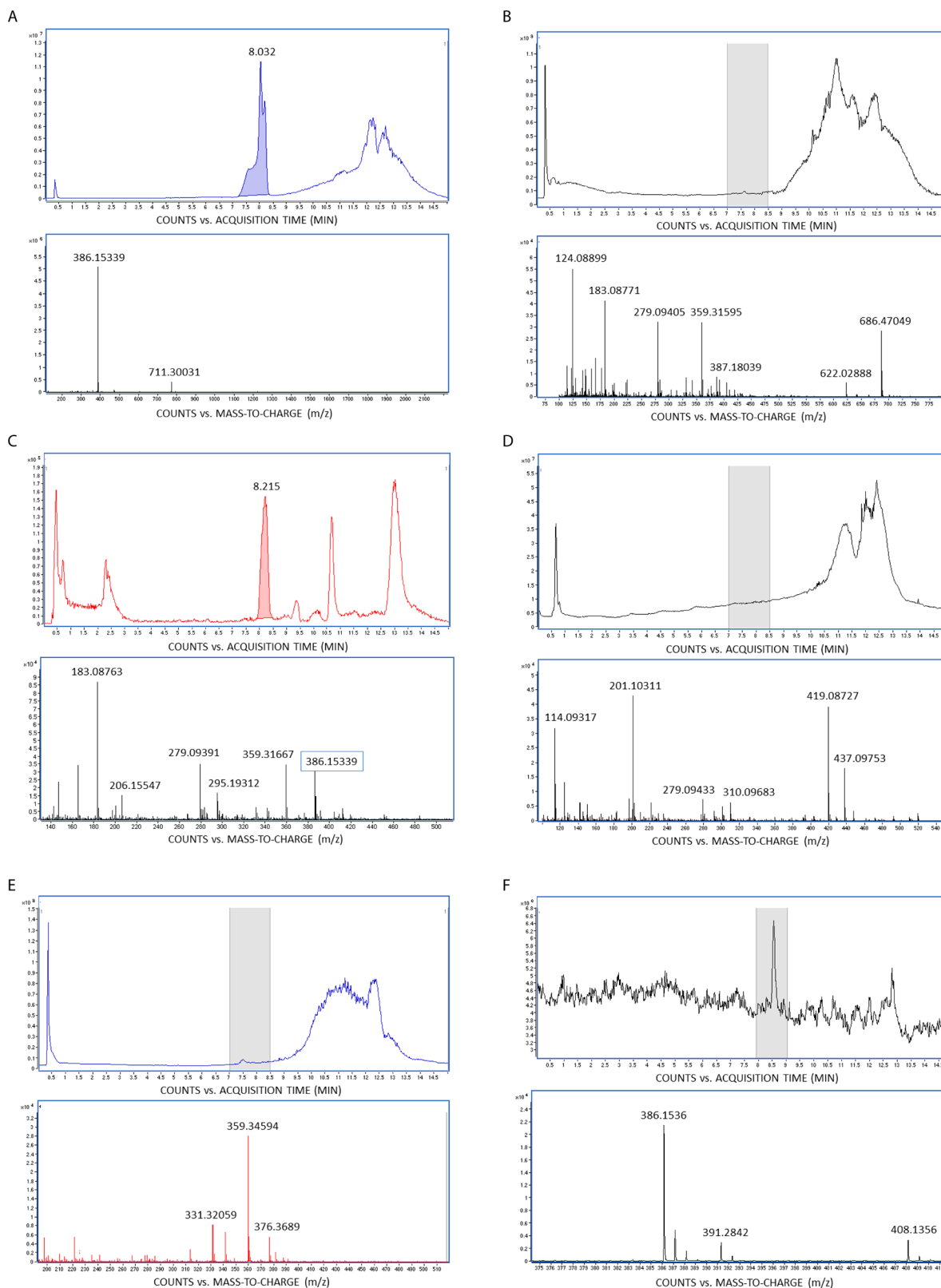
Figure 2. PP11 selectively localizes in mitochondria. Subcellular localization of **PP11** was investigated via HPLC-HRMS analysis of samples from different cellular compartments before and after treatment with the compound. (A) HPLC-HRMS profile of **PP11** analyzed in physiological solution revealed broad band absorption (7−8.5 min) with maximum absorption at a retention time of 8.03 min (top). Blue region of the HPLC spectrum corresponds to a unique mass peak at $[M + H]^+$ m/z of 386.15339 (bottom, $[M + H]^+$ calculated for **PP11** 386.1533). (B) HPLC profile of the mitochondrial fraction isolated from untreated cells revealed a relatively clean zone in the detection region of **PP11** (from 7 to 8.5 min, top). Gray band on the HPLC spectrum corresponds to the mass spectra area between a retention time of 7 and 8.5 min enlarged in the bottom panel. (C) HPLC-HRMS profile of the mitochondrial fraction isolated from cells pretreated with **PP11** clearly indicated the presence of the **PP11** compound with an HPLC band at a retention time of 8.2 min (top). Red area of the signal corresponds to the enlarged TIC signal for the mass

Figure 2. continued

peaks (bottom panel), among which the [M + H]$^+$ m/z of 386.15339 indicated that the presence of **PP11** was not detectable in the corresponding untreated fraction (B). (D) No detectable amount of **PP11** was found by HPLC-HRMS in the cytosolic fraction of **PP11**-treated cells. (E) HPLC profile of the ER fraction isolated from **PP11**-treated cells revealed a relatively clean zone in the detection region of **PP11** (from 7 to 8.5 min, top). Gray band of the HPLC spectrum corresponds to enlargement of the TIC signals of mass peaks detected by HRMS analysis (bottom). (F) HPLC-HRMS profile of the supernatant fraction isolated from cells pretreated with **PP11** indicated the presence of the compound.
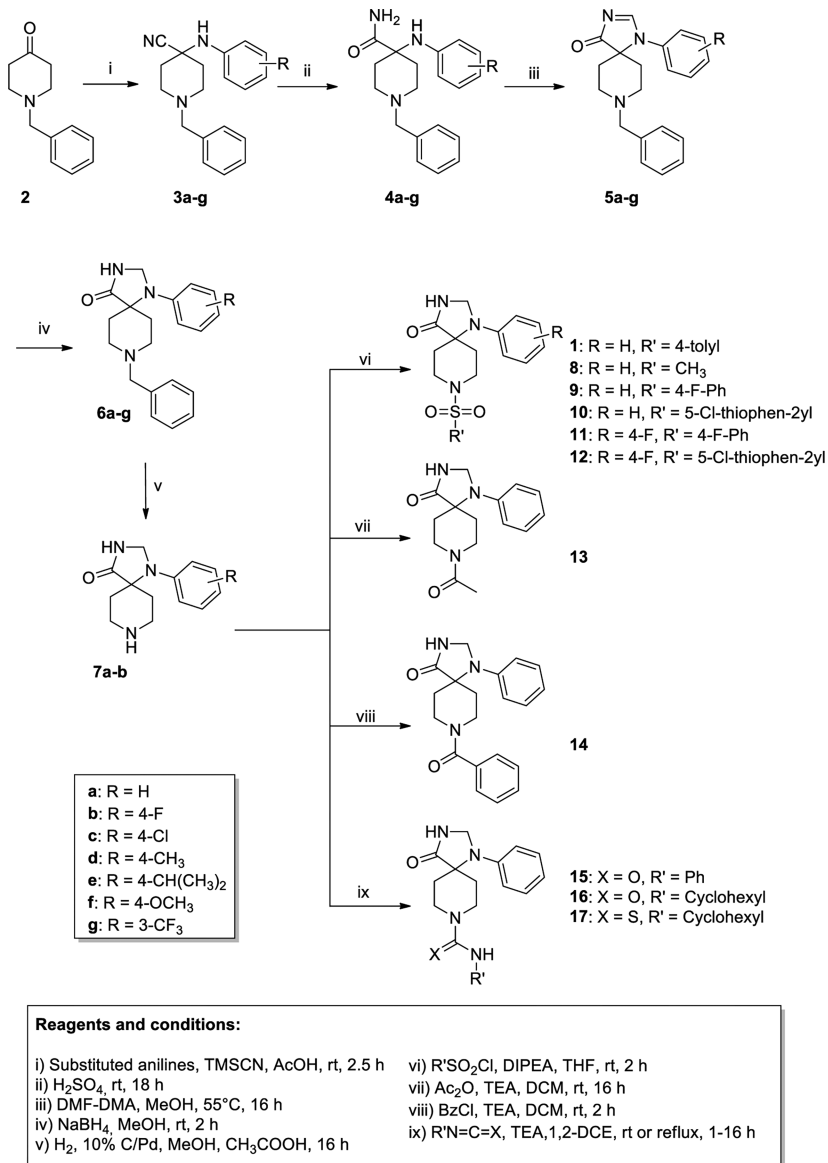

1: R = H, R' = 4-tolyl
8: R = H, R' = CH$_3$
9: R = H, R' = 4-F-Ph
10: R = H, R' = 5-Cl-thiophen-2yl
11: R = 4-F, R' = 4-F-Ph
12: R = 4-F, R' = 5-Cl-thiophen-2yl

13

14

15: X = O, R' = Ph
16: X = O, R' = Cyclohexyl
17: X = S, R' = Cyclohexyl

a: R = H
b: R = 4-F
c: R = 4-Cl
d: R = 4-CH$_3$
e: R = 4-CH(CH$_3$)$_2$
f: R = 4-OCH$_3$
g: R = 3-CF$_3$

Reagents and conditions:

i) Substituted anilines, TMSCN, AcOH, rt, 2.5 h
ii) H$_2$SO$_4$, rt, 18 h
iii) DMF-DMA, MeOH, 55°C, 16 h
iv) NaBH$_4$, MeOH, rt, 2 h
v) H$_2$, 10% C/Pd, MeOH, CH$_3$COOH, 16 h

vi) R'SO$_2$Cl, DIPEA, THF, rt, 2 h
vii) Ac$_2$O, TEA, DCM, rt, 16 h
viii) BzCl, TEA, DCM, rt, 2 h
ix) R'N=C=X, TEA, 1,2-DCE, rt or reflux, 1-16 h

Figure 3. Synthesis of PP11 and related spiro bicyclic derivatives.

■ RESULTS

Identification of 1-Phenyl-8-tosyl-1,3,8-triazaspiro[4.5]decan-4-one (PP11) as a Novel Small-Molecule Inhibitor of the mPTP. Oligomycin A is classified as an mPTP opening inhibitor that targets the c subunit of F$_1$/F$_O$-ATP synthase;[25] therefore, it was selected as the reference compound for this project. Indeed, oligomycin A is known to establish several van der Waals interactions with c subunits, forming a hydrogen bond with Glu[59] through a water molecule bridge through which the carboxyl group of a leucine residue is also recruited (Figure 1A).[24] In particular, the southern part of oligomycin A (Figure 1B) is closely engaged by the binding

cavity of the c ring.[24] Considering this information and the need to simplify this natural compound to facilitate easy, accessible synthesis, we explored the activity of a series of small molecules mimicking the southern 1,7-dioxaspiro[5.5]-undecane moiety of oligomycin A. To test the hypothesis that the spiro bicyclic fragment may be mandatory for mPTP inhibition, we initially screened a small internal library of spiro derivatives that somewhat resembles the functional structure of the natural compound. These preliminary investigations resulted in the identification of 1-phenyl-1,3,8-triaza-spiro-[4,5]decan-4-one derivative **1** (**PP11**, Figure 1C). To assess the efficacy of **PP11** in inhibiting Ca^{2+}-mediated mPTP opening, we first measured its biological activity in HeLa cells
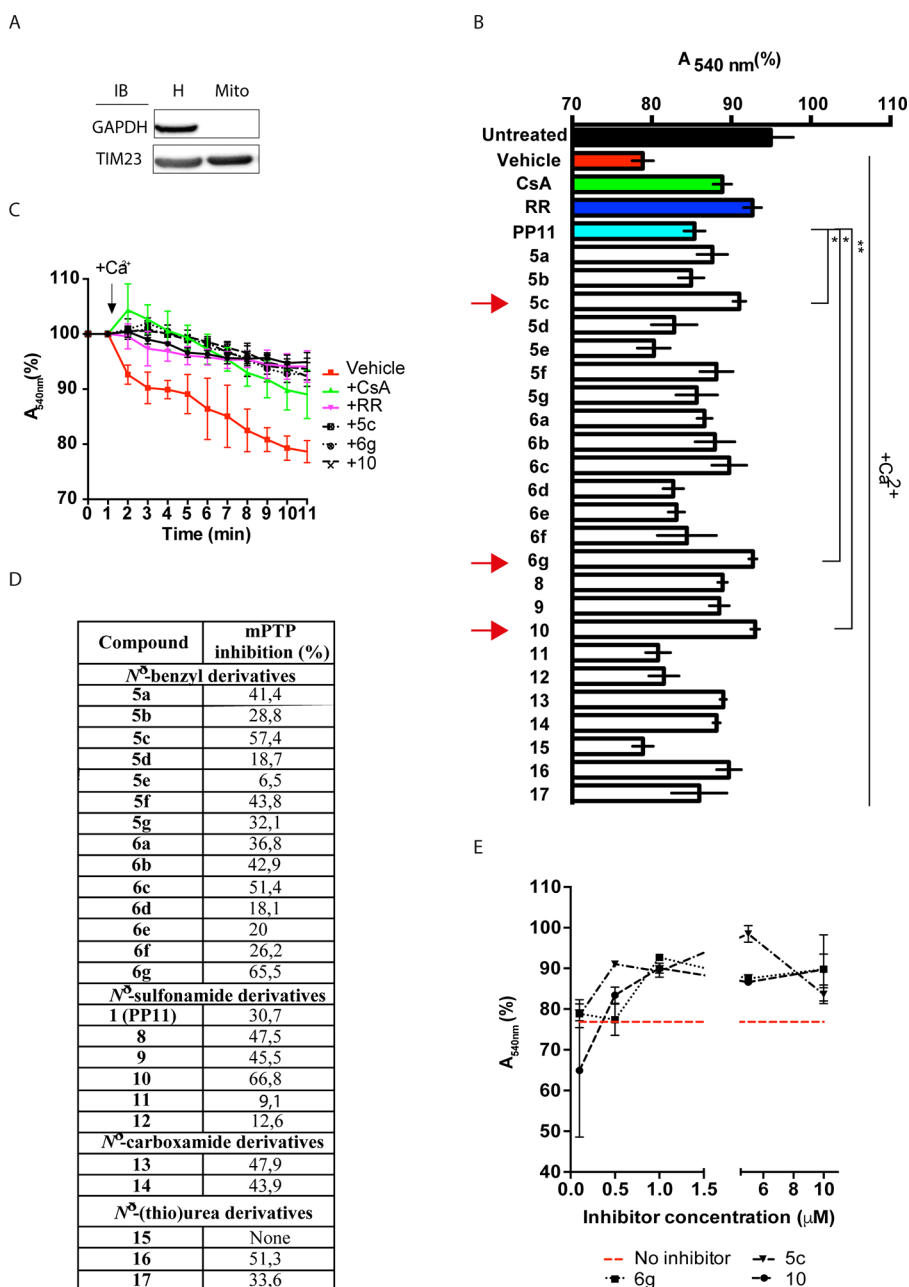
Figure 4. Screening of PP11 analogs. (A) Immunoblot detection of GAPDH (cytosolic marker) and TIM23 (mitochondrial marker) proteins in the homogenate (H) of the whole liver and in the mitochondrial (Mito) fraction. (B) Mitochondrial swelling assay for the screening of compounds in freshly isolated mouse liver mitochondria. Data were obtained by recording changes in absorbance (540 nm), and then the data were converted into percentages: (black bar) untreated and unstimulated mitochondria; (red bar) untreated mitochondria stimulated with 500 μM Ca^{2+}; (green bar) pretreatment with 1 μM CsA and stimulation with 500 μM Ca^{2+}; (blue bar) pretreatment with 5 μM RR and stimulation with 500 μM Ca^{2+}; (cyan bar) pretreatment with 1 μM **PP11** and stimulation with 500 μM Ca^{2+}; (white bars) pretreatment with 1 μM **PP11** analogs and stimulation with 500 μM Ca^{2+}. Red arrows indicate the three selected compounds. (C) Kinetics and statistical data from the mitochondrial swelling assay for the vehicle, CsA, RR, **5c**, **6g**, and **10** experimental conditions. (D) Mean percentages of mPTP inhibition with the tested compounds. (E) Dose−responses for the **5c**, **6g**, and **10** compounds. One-way ANOVA was used for statistical analysis; (*) p value < 0.05; (**) p value < 0.01. CsA: cyclosporine A. RR: ruthenium red.

by calcein−cobalt assay.[26] mPTP opening was stimulated by the addition of the ionophore ionomycin, and the resulting kinetics were compared. As shown in Figure 1D, the addition of 1 μM ionomycin to cells pretreated with 1 μM **PP11** resulted in desensitization of mPTP opening by approximately 50% as assessed by the slope of the curve after stimulation, which was significantly less than that observed in vehicle-treated cells. Moreover, **PP11** was able to inhibit the mPTP

opening in a manner very similar to that of oligomycin A[24,27,28] as a direct derivative but at a 10-fold lower concentration. These data demonstrated that the small-molecule inhibitor derived from the known compound oligomycin A was able to efficiently inhibit mPTP opening. Therefore, **PP11** was selected as the starting point for further studies.

PP11 Accumulates Selectively in Mitochondria. To monitor and better characterize **PP11**'s biological activity in
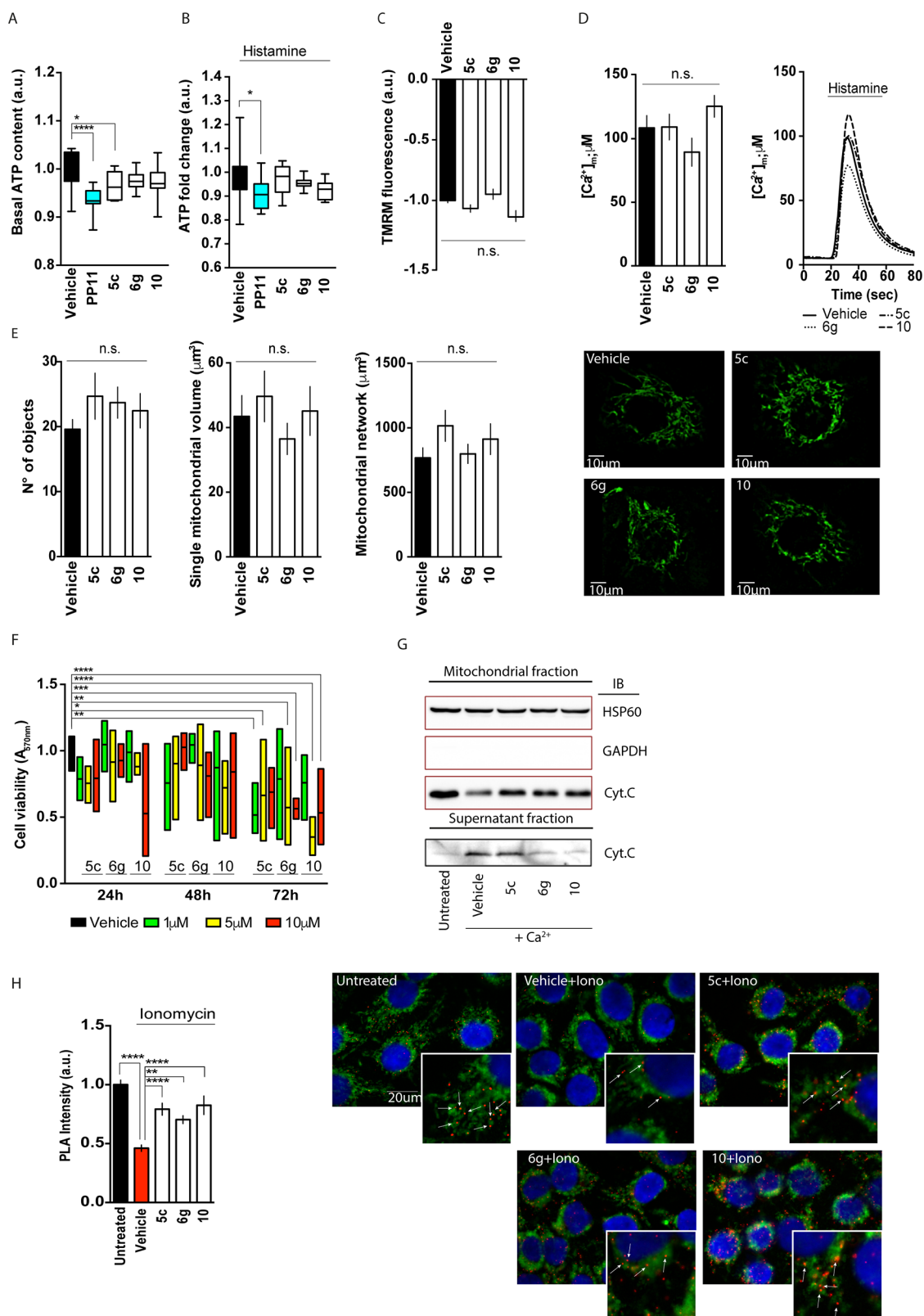
Figure 5. Biological profile of the most promising compounds. (A) Mitochondrial ATP content in living cells at resting conditions using the luciferase−luciferin method. (B) Mitochondrial ATP generation upon agonist-induced Ca^{2+} uptake in living cells using the luciferase−luciferin method. His indicates 100 μM histamine, the agonist used to induce Ca^{2+}-dependent ATP production. (C) TMRM fluorescence as an index of mitochondrial membrane potential changes in living cells. (D) Mitochondrial calcium uptake in living cells using a mitochondrially targeted aequorin probe; histograms of statistical and representative kinetics data; 100 μM histamine (His) addition is indicated. (E) Evaluation of mitochondrial morphology parameters using an mtCHERRY probe. (F) MTT assay in living cells to evaluate the toxicity of compounds at 24, 48, and 72 h and at different concentrations: (black bar) cells treated with vehicle; (green bar) 1 μM compound; (yellow bar) 5 μM; (red bar) 10 μM. Data were standardized to the vehicle condition. (G) Immunoblot detection of cytochrome c in both mitochondrial cristae and respiration buffer

Figure 5. continued

from the mitochondrial swelling assay. HSP60 was used as a mitochondrial marker, and GAPDH was used as a cytosolic marker. (H) PLA-based assay for assessment of the ATP synthase dimerization status: (blue) nuclei by DAPI detection; (green) mitochondria by TOM20 detection; (red spots) ATP5H detection as described in the methods. Representative images are shown below. au: arbitrary units. CytC: cytochrome *c*. n.s: not significant. (*) *p* value < 0.05. (**) *p* value < 0.01. (****) *p* value < 0.0001. IB: immunoblotting.

cells, we investigated its subcellular localization, focusing on the amount localized within mitochondria, the hypothetical site of action. As illustrated in Figure S1A−C, fractionation[29] of living cells treated with vehicle (A) or **PP11** (B) resulted in successful isolation of pure mitochondrial, cytosolic, and endoplasmic reticulum (ER) fractions. Samples from each subcellular compartment were analyzed by HPLC-HRMS to detect the compound. As shown in Figure 2C, **PP11** selectively accumulated in the mitochondria without detectable traces in the other subcellular fractions (Figure 2D and 2E); however, a residual amount of the spiro derivative was detectable in the supernatant fraction (Figure 2F). The same investigation performed after administration of oligomycin A (Figure S1C) revealed a less selective distribution of the compound with significant amounts detected in all of the isolated subcellular compartments (Figure S2).

Moreover, to directly monitor target engagement inside cells, we performed a cellular thermal shift assay (CETSA)[30,31] using a protocol based on ligand-induced thermal stabilization of the target protein, the c subunit of F_O-ATP synthase. Thermal shifts at high compound concentrations are known to correlate with median inhibitory concentration (IC_{50}) values and affinities, as measured by other methods;[32,33] therefore, by using higher concentrations of **PP11**, we were able to detect its binding with the c subunit of F_O-ATP synthase (Figure S1D) between 60 and 80 °C. Despite the low sensitivity of the assay and an inability to perform any molecular docking assays, Figure S1D shows that the c subunit protein was thermally stabilized by **PP11** pretreatment (red-dashed line) and that this effect was absent in other mitochondrial proteins, such as ATP5A (black-dashed line). To further confirm the putative selective **PP11**-c subunit binding, a UPLC-XEVO-TQD (Waters, UK) mass spectrometry investigation of the c subunit protein overexpressed in and immunoprecipitated from isolated mitochondria of **PP11**-pretreated cells was performed. The results from this experiment are reported in Figure S3 and indicate that a significant amount of **PP11** was clearly detectable and bound to the c subunit.

Together, these data confirm the ability of **PP11** to selectively enter mitochondria and bind the c subunit to inhibit mPTP opening.

Design, Synthesis, and Biological Characterization of PP11 Analogs as Inhibitors of the mPTP. Encouraged by the promising biological profile of **PP11** and considering the higher chemical stability of the aza-spiro moiety compared with the spiro-ketal function of oligomycin A, we initiated an SAR investigation of a new bicyclic core to improve compound potency. We applied a versatile synthetic approach that resulted in a series of **PP11** derivatives that were differentially substituted at the N^1 and N^8 positions (Figure 3). We first investigated the effect of replacing the tosyl function at the N^8 position of **PP11** with a benzyl group (compound **6a**) or with different sulfonamide (**8−10**), carboxamide (**13, 14**), urea (**15** and **16**), or thiourea (**17**) moieties. The results of the biological assay indicated that the compounds with the benzyl group or (hetero)arylsulfonamide N^8 substitutions exhibited

the best performance; these compounds were therefore combined with N^1 phenyl rings at the para/meta positions with both electron-donating or -withdrawing groups (compounds **6b−g**, **11**, and **12**). The common synthetic pathway for the preparation of all of the investigated final compounds is depicted in Figure 3. α-Aminonitriles **3a−g** were synthesized by a Strecker reaction from the commercially available *N*-benzylpiperidone **2**, which was reacted with (substituted) anilines in the presence of trimethylsilyl cyanide (TMSCN). The nitrile group was then hydrolyzed to the corresponding amide function (**4a−g**) by treatment with concentrated sulfuric acid. Spirocyclization was then performed with dimethylformamide dimethyl acetal (DMF-DMA), which resulted in generation of the unsaturated intermediates **5a−g**. The latter derivatives were also screened as mPTP inhibitors to evaluate the effect of the $C^2−N^3$ double bond constraining the 5-membered ring of the bicyclic template. Subsequently, the imidazolinone ring was efficiently reduced with $NaBH_4$ to yield the final compounds **6a−g**. Debenzylation at the N^8 position of **6a** and **6b** was performed via hydrogenation under Pd/C catalysis and yielded **7a** and **7b**, respectively, which were employed as key intermediates for the selective functionalization of the N^8 position. Specifically, the sulfonamide derivatives **1** and **8−12** were obtained by treatment of **7a** and **7b** with appropriate sulfonyl chlorides, while N^8 acetylation (**13**) or benzoylation (**14**) was achieved by standard treatment with acetic anhydride or benzoyl chloride, respectively. In addition, the urea derivatives **15** and **16** and the thiourea **17** were prepared from **7a** and the properly substituted isocyanates or isothiocyanates.

To investigate the effectiveness of the new, synthesized **PP11** analogs against mPTP opening, we used the mitochondrial swelling assay as previously described;[34] this protocol is faster than microscopy analysis for the screening of multiple compounds. **PP11** significantly inhibited mPTP opening (Figures 1D and 4B). To demonstrate specificity in measuring Ca^{2+}-induced mPTP opening, we added two positive controls, CsA and ruthenium red (RR), a known mPTP inhibitor and a mitochondrial calcium uptake blocker, respectively. Freshly isolated mouse liver mitochondria were first evaluated to ensure high purity (Figure 4A) and were then stimulated with 500 μM Ca^{2+}, and absorbance at 540 nm, at which a decrease was indicative of swelling, was monitored for 10 min (Figure 4B and 4C). Under these conditions, mitochondria treated with vehicle exhibited marked membrane swelling (red bar), which was significantly prevented by pretreatment with 1 μM CsA and 5 μM RR (green and blue bars, respectively). As shown in Figure 4B, most of the small molecules showed good inhibitory potential compared to the control mitochondrial sample (red bar). In particular, compounds **5c**, **6g**, and **10** were significantly more potent than **PP11** in inhibiting mPTP opening. Additional details are shown in Figure 4D, including the mean percentages of mPTP inhibition. Figure 4E shows that 1 μM was the lowest dose with the best effectiveness in inhibiting mitochondrial swelling for each selected compound.
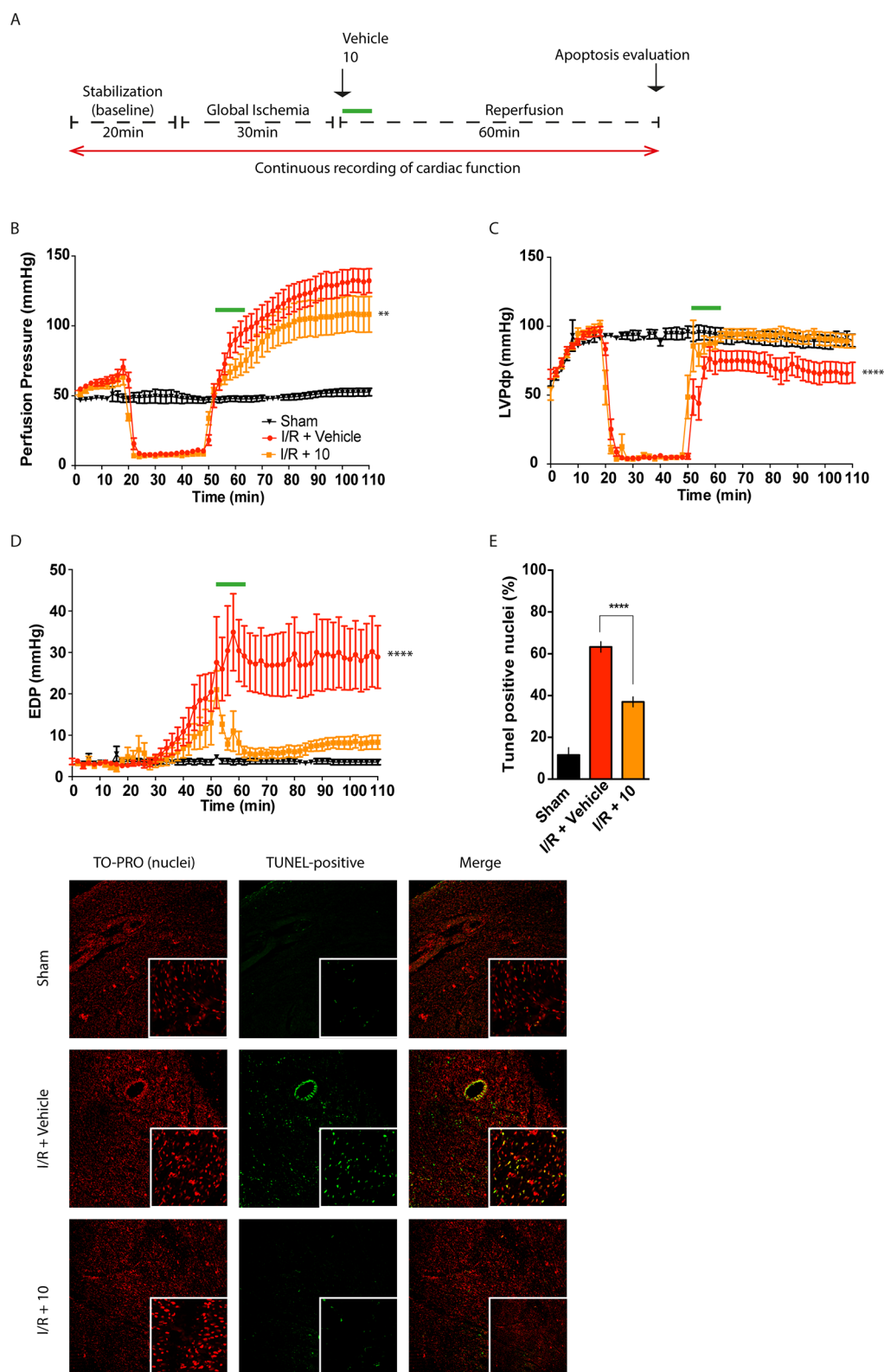
Figure 6. Beneficial effects of compound **10** in a cardiac reperfusion injury model. (A) Diagram depicting the standard Langendorff ex vivo protocol. (B) Coronary perfusion pressure recording of a rat heart in the stabilization, ischemia, and reperfusion phases. Compound **10** is used at a concentration of 10 μM. (C) Left ventricular peak developed pressure recording of a rat heart in the stabilization, ischemia, and reperfusion phases. (D) End-diastolic pressure recording of a rat heart in the stabilization, ischemia, and reperfusion phases. (E) TUNEL assay for apoptosis evaluation under experimental conditions and representative images: (red) nuclei detected by TO-PRO; (green) apoptotic nuclei detected by TUNEL enzyme. (**) p value < 0.01. (****) p value < 0.0001. Green bar in A−D indicates vehicle or compound administration time.

Biological Profile of the Most Promising Compounds.

Overall, mPTP assays revealed a set of three very potent inhibitors (**5c**, **6g**, and **10**) with the greatest effects on reducing mitochondrial swelling (Figure 4B) compared to **PP11**.

Given the crucial role of the c subunit in ATP synthase assembly and cellular energy production as a component of the membrane rotor, the basal mitochondrial ATP content and agonist-induced ATP production were monitored by the luciferin−luciferase assay.[35] Treatment of living cells with 1 μM **PP11** slightly but significantly depleted mitochondrial ATP levels in resting conditions (Figure 5A); similarly, the relative amount of ATP remained low even upon histamine-induced calcium uptake[36] (Figure 5B). The **PP11** derivatives **5c**, **6g**, and **10** synthesized with various specific chemical groups, such as electron-withdrawing atoms (Cl) or moieties (CF$_3$) in the aromatic substituents in positions 1 and 8 of the spirodecane scaffold, allowed us to successfully overcome this drawback and step-limiting factor. Indeed, use of the **6g** and **10** inhibitors did not affect ATP levels, but treatment with compound **5c** induced a small decrease in the basal mitochondrial ATP content, which was completely recovered upon Ca^{2+}-induced ATP generation (Figure 5A and 5B).

To identify possible side effects of the compounds on living cells that may preclude their use in future studies, we evaluated other important mitochondrial parameters. Mitochondrial membrane potential (MMP) and calcium homeostasis are critical factors for the maintenance of physiological functions in cells, including proper respiratory chain function and a wide range of intracellular signaling pathways, respectively. As shown in Figure 5C and 5D, pretreatment of cells with the **5c**, **6g**, and **10** inhibitors did not affect basal MMP or mitochondrial calcium uptake. Moreover, mitochondrial morphology, the number of mitochondria in cells, and their network volume were unchanged (Figure 5E).

In addition, the results previously described were further confirmed by the 3-(4,5-Dimethylthiazol-2-yl)-2,5-diphenylte-trazolium bromide (MTT) assay, which showed that treatment of living cells with micromolar concentrations of **5c**, **6g**, and **10** for 24 and 48 h did not induce significant MTT reduction compared with treatment with vehicle (Figure 5F). Only prolonged (72 h) treatment slightly but significantly decreased cell viability in vitro (Figure 5F).

The permeability transition pore has been postulated to play an important role in cytochrome c (CytC) release;[37] therefore, we explored the ability of the selected compounds to prevent CytC release from mitochondrial cristae. To correlate mPTP desensitization with apoptotic cell death prevention, we detected the amount of CytC in the cristae of mitochondrial fractions from the mitochondrial swelling assay upon calcium stimulation. Pretreatment with **5c**, **6g**, and **10** prevented CytC release as assessed by immunoblot analysis (Figure 5G). Taken together, these findings demonstrated that inhibition of mPTP opening may inhibit CytC release to the cytosol and consequently prevent apoptotic cell death (Figure 6E).

Next, to understand the molecular mechanism by which the selected compounds inhibit mPTP complex activity, we used a previously tested proximity ligation assay (PLA)-based procedure[10] to verify the F$_1$/F$_O$-ATP synthase dimerization grade in living cells. Vehicle-treated cells exhibited a considerable amount of red-dotted staining that colocalized with the mitochondrial protein translocase of outer mitochondrial membrane 20 (TOMM20). We showed the F$_1$/F$_O$-ATP synthase dimerization status via a PLA intensity profile upon ionomycin administration alone or in the presence of small-molecule inhibitors. As recently published by our lab, the MPT was accompanied by a significant decrease in the PLA signal following 1 μM ionomycin treatment;[10] however, the MPT did

not occur with the same intensity in the presence of 1 μM **5c**, **6g**, and **10** (Figure 5H). These findings suggest that mPTP desensitization by the synthesized compounds is correlated with stabilization of F$_1$/F$_O$-ATP synthase dimers.

Cardioprotective Effect of Compound 10 in a Model of Reperfusion Injury. Considering the ability of these inhibitors to desensitize mPTP opening (Figure 4B) by stabilizing ATP synthase dimers (Figure 5H) and prevent CytC release (Figure 5G) without affecting long-term cell viability (Figure 5F) and the mitochondrial ATP content (Figure 5A and 5B), we investigated the effects of compound **10** in an animal model of cardiac reperfusion injury. We isolated beating rat hearts and placed them in a Langendorff system, which was continuously perfused with Krebs−Henseleit buffer (KHB) bubbled with oxygen at 37 °C. The ex vivo protocol included stabilization of the heart for 20 min, and then retrograde perfusion was progressively stopped to induce 30 min of global ischemia followed by 1 h of reperfusion (Figure 6A). After stabilization, the left ventricular developed pressure (LVDP) was 89.8 ± 3 mmHg in the I/R vehicle group. Following reperfusion, the LVDP decreased to 66 ± 5 mmHg, with a mean reduction of 36 ± 9%, indicating successful induction of ischemia (as previously reported ref 38). No difference in LVDP was identified among the experimental groups during stabilization. As indicated in Figure 6A, compound **10** was administered in the reperfusion phase during the first 10 min of reflow. The dose of 10 μM of compound **10** was selected based on previous experiments to identify the highest dose that could be perfused in the heart without toxicity (data not shown). In isolated hearts, perfusion with a constant volume of derivative **10** resulted in decreases in coronary perfusion pressure (CPP) (−17.5 ± 3.4%) and end-diastolic pressure (EDP) (−72 ± 9.86%) (Figure 6B and 6D) with an increase in LVDP (+36.4 ± 3.9%) (Figure 6C), indicating reduced diastolic stiffness, vasoconstriction, and deterioration of myocardial performance, respectively. At the end of the procedure, cell death was analyzed in the hearts by terminal deoxynucleotidyl transferase dUTP nick-end labeling (TUNEL) assays. In the I/R+vehicle group, 64% of the cardiomyocytes were TUNEL positive; however, the number of TUNEL-positive cardiomyocytes was significantly reduced in the presence of spiro derivative **10** (Figure 6E).

These findings confirmed the ability of c-ring-targeting agents to inhibit mPTP opening and to protect against cell death in a cardiovascular model.

■ DISCUSSION AND CONCLUSIONS

Myocardial infarction is an ischemic heart disease in which mPTP opening is widely accepted as a crucial step in the development of myocardial damage, which is better known as ischemia−reperfusion injury (IRI).[6] Since up to 50% of the final infarct size is due to IRI, targeting the mPTP complex may be a valuable pharmacological adjunct to reduce infarct size. Currently, although satisfying results have been achieved in in vitro and in vivo animal models, manipulation of the PTPC and, more generally, mitochondrial targeting do not appear to influence the mortality of affected patients, but they reduce hospital readmission for heart failure.[39] Instead, drugs with a broad-spectrum mechanism of action are currently utilized in clinical practice.[39,40] The apparent lack of translational value among mitochondrial-targeting drugs can be ascribed first to limited knowledge regarding the exact molecular structure of mPTP; therefore, the appropriate

mitochondrial target possibly has not yet been considered. Second, the multifactorial nature of MI should be considered, and the adoption of combined strategies targeting multiple intracellular signaling pathways is always recommended.[41]

On the basis of our previous studies on the role of the c ring in mPTP opening[9,10] and to validate a new pharmacological approach for the treatment of ischemia−reperfusion-related damage, in this manuscript, we describe the discovery, optimization, and SAR studies of the first small-molecule mPTP opening inhibitors that target the c subunit of the F_1/F_O-ATP synthase complex.

To the best of our knowledge, this is the first attempt to inhibit the mPTP by targeting the eukaryotic c subunit of ATP synthase using novel small molecules for therapeutic purposes. Indeed, treatment during reperfusion with one of the most promising screened compounds (10) showed beneficial effects in an ex vivo model of MI, with a reduction of apoptotic cell death upon IRI (Figure 6E). The decreases in CPP and EDP (Figure 6B and 6D) with an increase in LVDP (Figure 6C) in the isolated heart reflected significant reductions in diastolic stiffness, vasoconstriction, and deterioration of myocardial performance. Moreover, the ex vivo beneficial effects of compound 10 together with strong inhibition of mPTP opening by the selected compounds in vitro can be achieved without altering mitochondrial parameters (Figure 5A−E) or short-term toxicity in living cells. Indeed, these compounds weakly but significantly disrupted cell viability only with 72 h of treatment (Figure 5F).

The compounds were derived using the scaffold of the known c subunit inhibitor oligomycin A; we first identified PP11, a compound with a strong desensitization effect on mPTP opening (Figure 1D) and an inhibitory effect comparable to that of oligomycin A, but it is functionally active at a 10-fold lower concentration (Figure 1D). The increased performance at lower concentrations can be ascribed to its better localization to the mitochondrial compartment (Figure 2), the putative site of action, as assessed by HPLC-HRMS. Indeed, PP11 accumulates exclusively in the pure mitochondrial fraction (Figure 2 and Figure S1) without detectable traces in other subcellular compartments. In contrast, although oligomycin A is present in the mitochondrial compartment where it exerts known biological effects, a significant amount diffuses into the cytoplasm and ER organelles (Figure S2), likely lowering its potency and conferring a better drug-like profile to PP11. In addition, given its effectiveness in targeting the c subunit for mPTP inhibition[9,10,14] and the exclusive mitochondrial localization of its ligand, PP11 (and derivatives) use led to fewer side effects compared to other known mPTP inhibitors, such as CsA. Indeed, CsA off-target effects[42,43] are derived from a diffuse intracellular localization pattern characterized by cytosolic[42,43] and nuclear interactions,[44] thus prompting research on alternative methods to target the mPTP.

Criticism could arise from the use of putative ATP synthase disruptors as ligands of the membrane rotor components, as confirmed in this work by the suboptimal effect of PP11, a preliminary derivative of oligomycin A, on the mitochondrial ATP content.[45] Indeed, although PP11 is considered a good mPTP opening inhibitor (Figure 1D), it has a slight deleterious effect on the production of basal ATP (Figure 5A); however, this effect is reduced upon Ca^{2+}-dependent stimulation in the mitochondria (Figure 5B). When designing PP11 derivatives, we tried to evaluate different chemical modifications at several positions of the parent compound to identify possible structural determinants that can abolish any undesired effects. Among the most promising compounds screened in Figure 4B, 6g and 10 did not affect the basal mitochondrial ATP content; only compound 5c promoted a small decrease in the basal mitochondrial ATP content, which was completely recovered upon Ca^{2+}-induced ATP generation. A possible explanation for such experimental evidence may be faster reversibility of the interaction of 6g and 10 with the postulated cellular target compared to PP11.

The main findings of this work are consistent with those of our previously published studies and those of independent groups,[12−14,46] confirming the importance of the roles of (i) the c ring as a core component in mPTP activity and (ii) the dimer versus monomer transition of ATP synthase linked to the mPTP and the resulting apoptotic cell death. Indeed, a PLA-dedicated assay suggested dimer stabilization upon Ca^{2+}-triggered mPTP opening when cells were pretreated with the 5c, 6g, and 10 compounds (Figure 5H) as a molecular mechanism by which these inhibitors may exert antiapoptotic effects.

We are aware that our data appear to disagree with the hypothesis from Walker's group on the persistence of the MPT in a cell clone lacking the c subunit of human ATP synthase;[47] however, as a very exhaustive commentary on this discrepancy explains,[48] in the absence of the primary mechanisms in mPTP opening (e.g., c subunit expression), the MPT can presumably occur through other pathways involving misfolded proteins of the mitochondrial membrane.[48,49]

In conclusion, we propose small-molecule c subunit inhibitors as a new pharmacological approach for the treatment of IRI. Future perspectives will be oriented toward the study of ATP synthase conformational changes (if detectable) in terms of modulation of its dynamic assembly into supercomplexes upon inhibitor treatment (for instance, by using native gels) and understanding the exact binding sites between inhibitors and mitochondrial protein(s). Photoaffinity labeling of the most promising compounds identified here may lead to useful tools that will facilitate future binding site deconvolution studies advancing structure-based drug design approaches in this field.

■ EXPERIMENTAL SECTION

Chemistry. Reaction progress and product mixtures were monitored by thin-layer chromatography (TLC) on silica gel (precoated F_{254} Macherey-Nagel plates) and visualized with a UV lamp (254 nm light source). The organic solutions from extractions were dried over anhydrous sodium sulfate. Chromatography was performed on Merck 230−400 mesh silica gel or using Isolera One (Biotage Sweden). ^1H, ^{13}C, DEPT, bidimensional (gCOSY), and heterocorrelated (gHMQC, gHMBC) NMR spectra were recorded on a VARIAN Mercury Plus 400 MHz spectrometer. Chemical shifts (δ) are reported in parts per million (ppm) using the peak of deuterated solvents as an internal standard, and coupling constants (J) are reported in Hertz. Splitting patterns are designed as follows: s, singlet; d, doublet; t, triplet; q, quartet; m, multiplet; and b, broad. Melting points for purified products were determined in a glass capillary on a Stuart Scientific electrothermal apparatus SMP3 and are uncorrected. Mass spectra were recorded by an ESI single-quadrupole mass spectrometer Waters ZQ 2000 (Waters Instruments UK). For analytical controls, Beckmann System Gold 168 HPLC was used with an LC column Kinetex 5-μm EVO C18 100 Å (250 × 4.6 mm) and a variable-wavelength UV detector fixed to 220 nm. The analysis was conducted using two solutions, A and B, containing 100:0.1 H_2O:TFA and 40:60:0.1 H_2O:CH_3CN:TFA, respectively, with a

gradient elution of 0−50% solution B over 30 min. The purity of all compounds was determined by HPLC and was greater than 95%.

LC-HRMS analysis of crude mitochondria and cytosol of PP11-treated cells and final compounds was performed with an ESI-Q-TOF Nano HPLC-CHIP Cube Agilent 6520 instrument (Agilent Technologies USA) using a linear gradient (0.4 μL/min) from 0% solvent A (97% water/3% acetonitrile/0.1% formic acid) to 80% solvent B (97% acetonitrile/3% water/0.1% formic acid) over 10 min and from 80% to 5% solvent B over 5 min using a Zorbax C18 Column (43 mm × 75 μm, 5 μm) equipped with an enrichment column (4 mm, 40 nL). The UPLC-MS analysis was performed in an Acquity UPLC equipped with a triple-quadrupole mass spectrometer XEVO-TQD (Waters UK). Chromatographic separation was carried out using a BHE C$_{18}$ column (50 mm × 2.1 mm i.d. 1.8 μm) from Waters (Waters, Milford, USA) heated at 40 °C. The mobile phase consisted of water with 0.1% formic acid (solvent A) and acetonitrile with 0.1% formic acid (Solvent B). An 8 min gradient elution at 0.3 mL/min was performed as follows: from 100% solvent A to 80% solvent A over 4 min, from 80% A to 20% A over 2 min, and from 20% A to 0% A over 2 min. Mass spectrometric detection was carried out using an electrospray interface (ESI) operated in positive ionization mode with multiple reaction monitoring (MRM) for the **PP11** analyte. Nitrogen was used as a desolvation gas at a 650 L/h flow rate with the desolvation temperature set at 200 °C and the source temperature set at 150 °C. The collision gas (argon) flow was set at 0.1 mL/min. The capillary voltage was set at 4 kV; the collision energy and con voltage were optimized to maximize the signal corresponding to the major transition observed in the MS/MS spectra following fragmentation of the $[M + H]^+$ ion corresponding to the **PP11** molecule.

Calcein−Cobalt Assay. HeLa cells were pretreated with DMSO (vehicle), 10 μM oligomycin A, 1 μM CsA, or 1 μM **PP11** and then loaded with calcein acetoxymethyl ester and Co^{2+} as previously described.[26] Staining solution was added to the cells for 15 min at 37 °C in a 5% CO$_2$ atmosphere. Image acquisitions were performed with a motorized Olympus IX81-ZDC inverted microscope with a 40 × /1.30-N.A. UPlanFLN oil-immersion objective and Cell MT20E xenon lamp. Ionomycin (1 μM) was administered 30 s after the beginning of the experiment to induce mPTP opening.

Mitochondrial Isolation and Swelling Assay. Mitochondria were isolated by conventional procedures involving differential centrifugation. Freshly excised SV129 mouse livers were washed and then homogenized in medium containing 50 mmol/L Tris-HCl, 25.67 g/L sucrose, and 40.98 g/L D-Mannitol (pH 7.4) supplemented with 0.5 mmol/L EGTA and 5 g/L bovine serum albumin (BSA). The homogenate was then transferred to microcentrifuge tubes and centrifuged at 0.8 rcf for 5 min for at least 2 cycles; the supernatants were collected, and the pellets were discarded. Subsequently, the sample was centrifuged at 10.0 rcf for 10 min to separate the mitochondrial fraction; the pellet was resuspended and ground in a loose-fitting glass Potter Elvehjem homogenizer for a fixed number of times. Samples were then centrifuged at 10.0 rcf for 10 min, and the pellet (mitochondria) was resuspended in 1 mL of Respiration Buffer (pH 7.4, Tris-HCl 50 mmol/L; 25.67 g/L sucrose; 40.98 g/L,D-Mannitol) supplemented with 5 mmol/L succinate. Mitochondria were quantified and diluted to a final concentration of 1 mg/mL for each mitochondrial swelling assay to monitor the changes in absorbance at 540 nm as previously described.[34] Incubations with small molecules were carried out at 25 °C, and mPTP opening was induced by the addition of 500 μM Ca^{2+}.

Ex Vivo Model. I/R was studied ex vivo using the Langendorff model with minor modifications.[10] In brief, upon euthanasia, the hearts of Wistar rats weighing 270−280 g at inclusion into the study were rapidly excised, immediately arrested in ice-cold KHB (pH 7.4; 4 °C), cannulated, and retrograde perfused at a fixed-flow rate (11 mL/min) through the aorta with warm KHB (37 °C) bubbled with 95% O$_2$ and 5% CO$_2$. Upon removal of the left atrial appendage, a latex fluid-filled balloon was inserted into the left ventricular chamber through the atrium to obtain an isovolumetrically beating preparation and connected to a pressure transducer (APT300, Hugo-Sachs,

Grünstrasse, Germany) by a fluid-filled polyethylene catheter to monitor performance. An additional transducer above the aortic cannula monitored the CPP. At the start of each experiment, the fluid in the balloon was increased incrementally to achieve a constant EDP of 4 ± 1 mmHg. The LVDP was then measured. The LVDP, EDP, and CPP were continuously recorded using a programmable acquisition system (HSE Isoheart Software for Isolated Heart, Hugo-Sachs, Grünstraße, Germany).

Proximity Ligation Assays. Cells were fixed in 4% PFA for 10 min at 37 °C, washed in PBS, placed in a jar containing 1 mmol/L EDTA buffer (pH 8.0) for 20 min at 100 °C (to improve epitope-antibody binding), and then placed at room temperature for an additional 10 min. Then the cells were permeabilized with 0.05% Triton X-100 for 10 min at 37 °C, and unspecific binding sites were blocked by incubating the cells in 0.05% Triton X-100 supplemented with 2% BSA for 45 min at 37 °C. Upon overnight incubation with ATP5H-specific antibodies that were previously conjugated to + or − PLA oligonucleotide probes per the instructions of the Duolink In Situ Probemaker kits, detection was performed as follows. A ligation−ligase solution was added to each sample for 30 min at 37 °C followed by 2 washes for 2 min each with Duolink In Situ Wash Buffer A; an amplification-polymerase solution was added and incubated for 100 min at 37 °C followed by 2 washes for 10 min each with 1× Duolink In Situ Wash Buffer B and 1 wash for 1 min with 0.01× Duolink In Situ Wash Buffer B. Cells were fixed again in 4% PFA for 10 min at 37 °C and then blocked in 0.05% Triton X-100 supplemented with 2% BSA for 10 min at 37 °C. Finally, the samples were incubated overnight with primary anti-TOM20 antibody, and the next day, the primary antibodies were revealed by incubation with the appropriate goat antirabbit Alexa Fluor 488 secondary antibodies. The slides were then stained with Duolink In Situ Detection Reagent Red and mounted using DAPI-containing Duolink In Situ Mounting Medium. Protein proximity was evaluated on an Axiovert 200 M fluorescence microscope equipped with a 40× water immersion objective (N.A. 1.2, from Carl Zeiss Microscopy, LLC) as a function of mitochondrial-localized red signal intensity.

Statistical Analysis. The statistical method included one-way ANOVA with multiple comparisons performed by GraphPad Prism. p values are reported in the figure legends.

■ ASSOCIATED CONTENT

Ⓢ Supporting Information

The Supporting Information is available free of charge on the ACS Publications website at DOI: 10.1021/acs.jmedchem.8b00278.

> Molecular formula strings for the final compounds **5a−g**, **1**, and **8−17** (CSV)
>
> Supplementary methods; general procedures for the preparation of compounds **3a−g**, **4a−g**, **5a−g**, **6a−g**, **7a−b**, **1**, and **8−17**; ^{1}H, ^{13}C, and DEPT NMR spectra of compounds **1**, **8−17**, and **6a−g**; HRMS spectra of compounds **5a−g**, **6a−g**, **1**, and **8−17** (PDF)

■ AUTHOR INFORMATION

Corresponding Authors

*E-mail: claudio.trapella@unife.it.
*E-mail: paolo.pinton@unife.it.

ORCID Ⓘ

Paolo Pinton: 0000-0001-7108-6508

Author Contributions

$^\$$G.M., D.P., and G.P. equally contributed to this manuscript.

Notes

The authors declare no competing financial interest.

■ ABBREVIATIONS USED

CETSA, cellular thermal shift assay; CsA, cyclosporine A; CPP, coronary perfusion pressure; CytC, cytochrome c; EDP, end-diastolic pressure; IMM, inner mitochondrial membrane; KRB, Krebs−Henseleit buffer; LVDP, left ventricular developed pressure; MI, myocardial infarction; MMP, mitochondrial membrane potential; MPT, mitochondrial permeability transition; PCD, programmed cell death; PLA, proximity ligation assay; PTPC, permeability transition pore complex; RR, ruthenium red; SAR, structure−activity relationship; TUNEL, terminal deoxynucleotidyl transferase dUTP nick-end labeling

■ REFERENCES

(1) Meier, P.; Finch, A.; Evan, G. Apoptosis in development. *Nature* **2000**, *407*, 796−801.

(2) Izzo, V.; Bravo-San Pedro, J. M.; Sica, V.; Kroemer, G.; Galluzzi, L. Mitochondrial permeability transition: new findings and persisting uncertainties. *Trends Cell Biol.* **2016**, *26*, 655−667.

(3) Bonora, M.; Wieckowsk, M. R.; Chinopoulos, C.; Kepp, O.; Kroemer, G.; Galluzzi, L.; Pinton, P. Molecular mechanisms of cell death: central implication of ATP synthase in mitochondrial permeability transition. *Oncogene* **2015**, *34*, 1608.

(4) Halestrap, A. P. A pore way to die: the role of mitochondria in reperfusion injury and cardioprotection. *Biochem. Soc. Trans.* **2010**, *38*, 841−860.

(5) Morciano, G.; Giorgi, C.; Bonora, M.; Punzetti, S.; Pavasini, R.; Wieckowski, M. R.; Campo, G.; Pinton, P. Molecular identity of the mitochondrial permeability transition pore and its role in ischemia-reperfusion injury. *J. Mol. Cell. Cardiol.* **2015**, *78*, 142−153.

(6) Ferrari, R.; Balla, C.; Malagu, M.; Guardigli, G.; Morciano, G.; Bertini, M.; Biscaglia, S.; Campo, G. Reperfusion damage - a story of success, failure, and hope. *Circ. J.* **2017**, *81*, 131−141.

(7) Giorgio, V.; Bisetto, E.; Soriano, M. E.; Dabbeni-Sala, F.; Basso, E.; Petronilli, V.; Forte, M. A.; Bernardi, P.; Lippe, G. Cyclophilin D modulates mitochondrial F0F1-ATP synthase by interacting with the lateral stalk of the complex. *J. Biol. Chem.* **2009**, *284*, 33982−33988.

(8) Shanmughapriya, S.; Rajan, S.; Hoffman, N. E.; Higgins, A. M.; Tomar, D.; Nemani, N.; Hines, K. J.; Smith, D. J.; Eguchi, A.; Vallem, S.; Shaikh, F.; Cheung, M.; Leonard, N. J.; Stolakis, R. S.; Wolfers, M. P.; Ibetti, J.; Chuprun, J. K.; Jog, N. R.; Houser, S. R.; Koch, W. J.; Elrod, J. W.; Madesh, M. SPG7 is an essential and conserved component of the mitochondrial permeability transition pore. *Mol. Cell* **2015**, *60*, 47−62.

(9) Bonora, M.; Bononi, A.; De Marchi, E.; Giorgi, C.; Lebiedzinska, M.; Marchi, S.; Patergnani, S.; Rimessi, A.; Suski, J. M.; Wojtala, A.; Wieckowski, M. R.; Kroemer, G.; Galluzzi, L.; Pinton, P. Role of the c subunit of the FO ATP synthase in mitochondrial permeability transition. *Cell Cycle* **2013**, *12*, 674−683.

(10) Bonora, M.; Morganti, C.; Morciano, G.; Pedriali, G.; Lebiedzinska-Arciszewska, M.; Aquila, G.; Giorgi, C.; Rizzo, P.; Campo, G.; Ferrari, R.; Kroemer, G.; Wieckowski, M. R.; Galluzzi, L.; Pinton, P. Mitochondrial permeability transition involves dissociation of F1FO ATP synthase dimers and C-ring conformation. *EMBO Rep.* **2017**, *18*, 1077−1089.

(11) Giorgio, V.; von Stockum, S.; Antoniel, M.; Fabbro, A.; Fogolari, F.; Forte, M.; Glick, G. D.; Petronilli, V.; Zoratti, M.; Szabo, I.; Lippe, G.; Bernardi, P. Dimers of mitochondrial ATP synthase form the permeability transition pore. *Proc. Natl. Acad. Sci. U. S. A.* **2013**, *110*, 5887−5892.

(12) Alavian, K. N.; Beutner, G.; Lazrove, E.; Sacchetti, S.; Park, H. A.; Licznerski, P.; Li, H.; Nabili, P.; Hockensmith, K.; Graham, M.; Porter, G. A., Jr.; Jonas, E. A. An uncoupling channel within the c-subunit ring of the F1FO ATP synthase is the mitochondrial permeability transition pore. *Proc. Natl. Acad. Sci. U. S. A.* **2014**, *111*, 10580−10585.

(13) Azarashvili, T.; Odinokova, I.; Bakunts, A.; Ternovsky, V.; Krestinina, O.; Tyynela, J.; Saris, N. E. Potential role of subunit c of F0F1-ATPase and subunit c of storage body in the mitochondrial permeability transition. Effect of the phosphorylation status of subunit c on pore opening. *Cell Calcium* **2014**, *55*, 69−77.

(14) Elustondo, P. A.; Nichols, M.; Negoda, A.; Thirumaran, A.; Zakharian, E.; Robertson, G. S.; Pavlov, E. V. Mitochondrial permeability transition pore induction is linked to formation of the complex of ATPase C-subunit, polyhydroxybutyrate and inorganic polyphosphate. *Cell Death Discov* **2016**, *2*, 16070.

(15) Morciano, G.; Bonora, M.; Giorgi, C.; Pinton, P. Other bricks for the correct construction of the mitochondrial permeability transition pore complex. *Cell Death Dis.* **2017**, *8*, e2698.

(16) Zorow, D. B.; Kinnally, K. W.; Perini, S.; Tedeschi, H. Multiple conductance levels in rat heart inner mitochondrial membranes studied by patch clamping. *Biochim. Biophys. Acta, Biomembr.* **1992**, *1105*, 263−270.

(17) Zhou, W.; Marinelli, F.; Nief, C.; Faraldo-Gomez, J. D. Atomistic simulations indicate the c-subunit ring of the F1Fo ATP synthase is not the mitochondrial permeability transition pore. *eLife* **2017**, *6*. DOI: 10.7554/eLife.23781

(18) Fancelli, D.; Abate, A.; Amici, R.; Bernardi, P.; Ballarini, M.; Cappa, A.; Carenzi, G.; Colombo, A.; Contursi, C.; Di Lisa, F.; Dondio, G.; Gagliardi, S.; Milanesi, E.; Minucci, S.; Pain, G.; Pelicci, P. G.; Saccani, A.; Storto, M.; Thaler, F.; Varasi, M.; Villa, M.; Plyte, S. Cinnamic anilides as new mitochondrial permeability transition pore inhibitors endowed with ischemia-reperfusion injury protective effect in vivo. *J. Med. Chem.* **2014**, *57*, 5333−5347.

(19) Martin, L. J.; Fancelli, D.; Wong, M.; Niedzwiecki, M.; Ballarini, M.; Plyte, S.; Chang, Q. GNX-4728, a novel small molecule drug inhibitor of mitochondrial permeability transition, is therapeutic in a mouse model of amyotrophic lateral sclerosis. *Front. Cell. Neurosci.* **2014**, *8*, 433.

(20) Yin, Y.; Guan, Y.; Duan, J.; Wei, G.; Zhu, Y.; Quan, W.; Guo, C.; Zhou, D.; Wang, Y.; Xi, M.; Wen, A. Cardioprotective effect of Danshensu against myocardial ischemia/reperfusion injury and inhibits apoptosis of H9c2 cardiomyocytes via Akt and ERK1/2 phosphorylation. *Eur. J. Pharmacol.* **2013**, *699*, 219−226.

(21) Lardy, H. A.; Johnson, D.; McMurray, W. C. Antibiotics as tools for metabolic studies. I. A survey of toxic antibiotics in respiratory, phosphorylative and glycolytic systems. *Arch. Biochem. Biophys.* **1958**, *78*, 587−597.

(22) Zhu, Y.; Xu, H.; Huang, K. Mitochondrial permeability transition and cytochrome c release induced by selenite. *J. Inorg. Biochem.* **2002**, *90*, 43−50.

(23) Chavez, E.; Rodriguez, J. S.; Garcia, G.; Garcia, N.; Correa, F. Oligomycin strengthens the effect of cyclosporin A on mitochondrial permeability transition by inducing phosphate uptake. *Cell Biol. Int.* **2005**, *29*, 551−558.

(24) Symersky, J.; Osowski, D.; Walters, D. E.; Mueller, D. M. Oligomycin frames a common drug-binding site in the ATP synthase. *Proc. Natl. Acad. Sci. U. S. A.* **2012**, *109*, 13961−13965.

(25) Hong, S.; Pedersen, P. L. ATP synthase and the actions of inhibitors utilized to study its roles in human health, disease, and other scientific areas. *Microbiol Mol. Biol. Rev.* **2008**, *72*, 590−641.

(26) Bonora, M.; Morganti, C.; Morciano, G.; Giorgi, C.; Wieckowski, M. R.; Pinton, P. Comprehensive analysis of mitochondrial permeability transition pore activity in living cells using fluorescence-imaging-based techniques. *Nat. Protoc.* **2016**, *11*, 1067−1080.

(27) Chinopoulos, C.; Szabadkai, G. What makes you can also break you: mitochondrial permeability transition pore formation by the c subunit of the F(1)F(0) ATP-synthase? *Front. Oncol.* **2013**, *3*, 25.

(28) Blanchet, L.; Grefte, S.; Smeitink, J. A.; Willems, P. H.; Koopman, W. J. Photo-induction and automated quantification of reversible mitochondrial permeability transition pore opening in primary mouse myotubes. *PLoS One* **2014**, *9*, e114090.

(29) Suski, J. M.; Lebiedzinska, M.; Wojtala, A.; Duszynski, J.; Giorgi, C.; Pinton, P.; Wieckowski, M. R. Isolation of plasma membrane-associated membranes from rat liver. *Nat. Protoc.* **2014**, *9*, 312−322.

(30) Jafari, R.; Almqvist, H.; Axelsson, H.; Ignatushchenko, M.; Lundback, T.; Nordlund, P.; Molina, D. M. The cellular thermal shift assay for evaluating drug target interactions in cells. *Nat. Protoc.* **2014**, *9*, 2100−2122.

(31) Molina, D. M.; Jafari, R.; Ignatushchenko, M.; Seki, T.; Larsson, E. A.; Dan, C.; Sreekumar, L.; Cao, Y.; Nordlund, P. Monitoring drug target engagement in cells and tissues using the cellular thermal shift assay. *Science* **2013**, *341*, 84−87.

(32) Fedorov, O.; Marsden, B.; Pogacic, V.; Rellos, P.; Muller, S.; Bullock, A. N.; Schwaller, J.; Sundstrom, M.; Knapp, S. A systematic interaction map of validated kinase inhibitors with Ser/Thr kinases. *Proc. Natl. Acad. Sci. U. S. A.* **2007**, *104*, 20523−20528.

(33) Wahlberg, E.; Karlberg, T.; Kouznetsova, E.; Markova, N.; Macchiarulo, A.; Thorsell, A. G.; Pol, E.; Frostell, A.; Ekblad, T.; Oncu, D.; Kull, B.; Robertson, G. M.; Pellicciari, R.; Schuler, H.; Weigelt, J. Family-wide chemical profiling and structural analysis of PARP and tankyrase inhibitors. *Nat. Biotechnol.* **2012**, *30*, 283−288.

(34) Di Lisa, F.; Menabo, R.; Canton, M.; Barile, M.; Bernardi, P. Opening of the mitochondrial permeability transition pore causes depletion of mitochondrial and cytosolic NAD+ and is a causative event in the death of myocytes in postischemic reperfusion of the heart. *J. Biol. Chem.* **2001**, *276*, 2571−2575.

(35) Morciano, G.; Sarti, A. C.; Marchi, S.; Missiroli, S.; Falzoni, S.; Raffaghello, L.; Pistoia, V.; Giorgi, C.; Di Virgilio, F.; Pinton, P. Use of luciferase probes to measure ATP in living cells and animals. *Nat. Protoc.* **2017**, *12*, 1542−1562.

(36) Jouaville, L. S.; Pinton, P.; Bastianutto, C.; Rutter, G. A.; Rizzuto, R. Regulation of mitochondrial ATP synthesis by calcium: evidence for a long-term metabolic priming. *Proc. Natl. Acad. Sci. U. S. A.* **1999**, *96*, 13807−13812.

(37) Baines, C. P.; Kaiser, R. A.; Purcell, N. H.; Blair, N. S.; Osinska, H.; Hambleton, M. A.; Brunskill, E. W.; Sayen, M. R.; Gottlieb, R. A.; Dorn, G. W.; Robbins, J.; Molkentin, J. D. Loss of cyclophilin D reveals a critical role for mitochondrial permeability transition in cell death. *Nature* **2005**, *434*, 658−662.

(38) Bell, R. M.; Mocanu, M. M.; Yellon, D. M. Retrograde heart perfusion: the Langendorff technique of isolated heart perfusion. *J. Mol. Cell. Cardiol.* **2011**, *50*, 940−950.

(39) Campo, G.; Pavasini, R.; Morciano, G.; Lincoff, A. M.; Gibson, C. M.; Kitakaze, M.; Lonborg, J.; Ahluwalia, A.; Ishii, H.; Frenneaux, M.; Ovize, M.; Galvani, M.; Atar, D.; Ibanez, B.; Cerisano, G.; Biscaglia, S.; Neil, B. J.; Asakura, M.; Engstrom, T.; Jones, D. A.; Dawson, D.; Ferrari, R.; Pinton, P.; Ottani, F. Clinical benefit of drugs targeting mitochondrial function as an adjunct to reperfusion in ST-segment elevation myocardial infarction: A meta-analysis of randomized clinical trials. *Int. J. Cardiol.* **2017**, *244*, 59−66.

(40) Campo, G.; Pavasini, R.; Morciano, G.; Lincoff, M. A.; Gibson, M. C.; Kitakaze, M.; Lonborg, J.; Ahluwalia, A.; Ishii, H.; Frenneaux, M.; Ovize, M.; Galvani, M.; Atar, D.; Ibanez, B.; Cerisano, G.; Biscaglia, S.; Neil, B. J.; Asakura, M.; Engstrom, T.; Jones, D. A.; Dawson, D.; Ferrari, R.; Pinton, P.; Ottani, F. Data on administration of cyclosporine, nicorandil, metoprolol on reperfusion related outcomes in ST-segment elevation myocardial infarction treated with percutaneous coronary intervention. *Data Brief* **2017**, *14*, 197−205.

(41) Hausenloy, D. J.; Yellon, D. M. Combination therapy to target reperfusion injury after ST-segment-elevation myocardial infarction: a more effective approach to cardioprotection. *Circulation* **2017**, *136*, 904−906.

(42) Abikhair, M.; Mitsui, H.; Yanofsky, V.; Roudiani, N.; Ovits, C.; Bryan, T.; Oberyszyn, T. M.; Tober, K. L.; Gonzalez, J.; Krueger, J. G.; Felsen, D.; Carucci, J. A. Cyclosporine A immunosuppression drives catastrophic squamous cell carcinoma through IL-22. *JCI Insight* **2016**, *1*, e86434.

(43) Youn, T. J.; Piao, H.; Kwon, J. S.; Choi, S. Y.; Kim, H. S.; Park, D. G.; Kim, D. W.; Kim, Y. G.; Cho, M. C. Effects of the calcineurin dependent signaling pathway inhibition by cyclosporin A on early and late cardiac remodeling following myocardial infarction. *Eur. J. Heart Failure* **2002**, *4*, 713−718.

(44) Le Hir, M.; Su, Q.; Weber, L.; Woerly, G.; Granelli-Piperno, A.; Ryffel, B. In situ detection of cyclosporin A: evidence for nuclear localization of cyclosporine and cyclophilins. *Lab Invest.* **1995**, *73*, 727−733.

(45) Matsuno-Yagi, A.; Hatefi, Y. Kinetic modalities of ATP synthesis. Regulation by the mitochondrial respiratory chain. *J. Biol. Chem.* **1986**, *261*, 14031−14038.

(46) Beutner, G.; Alanzalon, R. E.; Porter, G. A., Jr. Cyclophilin D regulates the dynamic assembly of mitochondrial ATP synthase into synthasomes. *Sci. Rep.* **2017**, *7*, 14488.

(47) He, J.; Ford, H. C.; Carroll, J.; Ding, S.; Fearnley, I. M.; Walker, J. E. Persistence of the mitochondrial permeability transition in the absence of subunit c of human ATP synthase. *Proc. Natl. Acad. Sci. U. S. A.* **2017**, *114*, 3409−3414.

(48) Amodeo, G. F.; Solesio, M. E.; Pavlov, E. V. From ATP synthase dimers to C-ring conformational changes: unified model of the mitochondrial permeability transition pore. *Cell Death Dis.* **2017**, *8*, 1.

(49) He, L.; Lemasters, J. J. Regulated and unregulated mitochondrial permeability transition pores: a new paradigm of pore structure and function? *FEBS Lett.* **2002**, *512*, 1−7.